Study of Tamm Plasmon

Dinesh Beniwal

Department of Physics, National Institute of Science Education and Research, India

E-mail: dinesh.beniwal@niser.ac.in

Abstract. Surface plasmon resonance can be supported by materials with a negative real and modest positive imaginary dielectric constant (SPR). Surface conduction electrons energised by electromagnetic (EM) radiation form a coherent oscillation in this resonance. The following experiment simulation concerns itself with the study of Surface States in periodic stratified medium (DBRs). The symmetry between the periodic potential in Condensed matter Physics and its optical analogue in terms of refractive indices is exploited to develop a theoretical framework. The varying of the nature of the DBR and its spectra obtained are varied with the simulation done under Python programming language.It was developed to extensively study the properties and conditions of Tamm Plasmon excitations and observance of Resonant wavelength in the Reflectivity spectrum.There is qualitative observation of Tamm state excitation and dependence of angle of incidence on Resonant wavelength for s and p-Polarisation.

Keywords: DBR (Distributed Bragg Reflectors), Tamm states, Surface plasmon resonance (SPR), Surface plasmon polariton (SPP)

1. Content

2. Light matter interaction

Maxwell's equations are used to derive the equations connected with surface plasmon waves. The production of electric and magnetic fields is explained using Maxwell's equations, which are the cornerstone of electromagnetic theory.

$$\nabla.D = \rho_f \tag{1}$$

$$\nabla.B = 0 \tag{2}$$

$$\nabla \times E = -\frac{\partial B}{\partial t} \tag{3}$$

$$\nabla \times H = J_f + \frac{\partial D}{\partial t} \tag{4}$$

D is the electric flux density, B is the magnetic flux density, E is the electric field, H is the magnetic field, $_f$ is the free charge density and J_f is the free current density. For homogeneous, isotropic and linear dielectric material, D and B can be related to E and H by:

$$D = \epsilon_o E + P = \epsilon_o \epsilon_r E \tag{5}$$

$$H = \frac{B}{\mu_o} - M = \frac{B}{\mu_o \mu_r} \tag{6}$$

where P is the polarisation, M is the magnetisation.

The Drude model, established by Paul Drude in 1900, argues that a lattice of positively charged ionic cores and negatively charged gas forms the metal. Plasma is a negatively charged gas that is created by ensemble conduction electrons travelling freely inside a metal. The optical characteristics of a metal are described using this paradigm. If a volume of plasma is displaced by a distance, x, it results in a polarisation, P. This leads to the formation of an electric field, E, with the following relationship:

$$E = -\frac{P}{\epsilon_o} = \frac{nex}{\epsilon_o} \tag{7}$$

After a solving maxwell's equation for this model we get:

$$D = \epsilon_o(1 - \frac{\omega_p}{\omega^2 + \iota w \omega_c})E \tag{8}$$

here The natural frequency of oscillation associated with the plasma is known as the plasma frequency (ω_p) and is defined as:

$$\omega_p = \sqrt{\frac{ne^2}{\epsilon_o m}} \tag{9}$$

At frequencies below the plasma frequency ($\omega < \omega_p$), the permittivity is negative and the metal is reflective in nature. At frequencies above the plasma frequency ($\omega > \omega_p$), the permittivity is positive and the metal becomes mainly absorbing.[1]

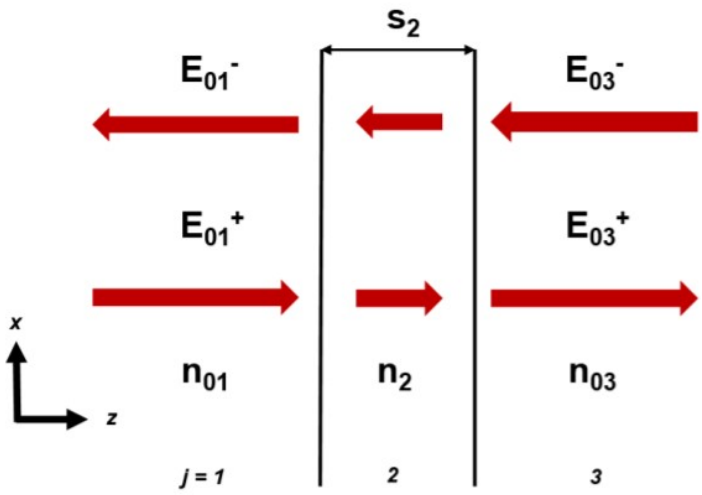

Figure 1: Diagram of a single layer structure [2]

3. Light in layered media

Waves propagating through layered media is a common occurrence in many areas of physics and several different methods have been developed to solve this problem such as the scattering matrix method or using recursive functions. The transfer matrix method (TMM) is a relatively simple technique that can be used to calculate the reflection, transmission and absorption coefficients of a structure consisting of a series of layers with different thicknesses and refractive indices.

3.1. ***The transfer matrix method (TMM)***

Let us consider the simplest such structure, consisting of one layer with thickness s_2 and complex refractive index n_2, positioned between two semi-infinite media with refractive index n_{01} and n_{03} (the ambient and substrate materials), and shown in Figure 1. As Maxwell's equations are linear, the electric field at any point can be described as the sum of the forward and backward propagating component.

$$E_j(z) = E_j^+(z) + E_j^-(z) \tag{10}$$

First, let us only consider how the electric field changes as it propagates through the single layer of thickness s_2. Each component will experience a change in phase (ϕ) that will be equal in magnitude but with opposite signs as they have opposite wave-vectors.

$$E_2(z) = E_2^+(z+s_2)e^{-i\Phi} + E_2^-(z+s_2)e^{i\Phi}$$

which can be written as a 2×2 matrix, called the propagation matrix (or layer matrix)

$$\vec{E}_2(z) = L_2\vec{E}_2(z+s_2) = \begin{bmatrix} e^{-i\Phi} & 0 \\ 0 & e^{i\Phi} \end{bmatrix} \vec{E}_2(z+s_2)$$

where $\vec{E}$ is a column vector of the amplitudes of the forward and backward travelling wave

$$\vec{E} = \begin{bmatrix} E^+ \\ E^- \end{bmatrix}$$

and

$$\Phi = n_2 \frac{\omega}{c} s_2 = \kappa_2 s_2$$

where s_2 gives the layer's thickness and $n_2(\omega/c)$ the spatial frequency (assuming normal incidence). The propagation matrix calculates the change in phase and amplitude after propagating through the layer, though if n_2 is purely real then there will be no absorption and it only describe a phase change.

Next, the effect of the interface is accounted for. Consider a single interface between two layers 1 and 2, and that has light incident on both sides. The reflection coefficient r_{ij} is the ratio of the reflected amplitude going from layer i to j to the incident amplitude, and t_{ij} the same for the transmitted amplitude. These are related by

$$E_1^- = r_{12}E_1^+ + t_{21}E_2^-$$

$$E_2^+ = t_{12}E_1^+ + r_{21}E_2^-$$

which can also be written as a 2×2 interface matrix

$$\vec{E}_1 = I_{1,2}\vec{E}_2 = \left(\frac{1}{t_{12}}\right) \begin{bmatrix} 1 & r_{12} \\ r_{12} & 1 \end{bmatrix} \vec{E}_2$$

The transfer matrix of a multilayer structure is a product of these two types of matrices; the propagation matrix and interface matrix. So in the case considered in Figure 2 the propagation through the whole structure can be described as the product of the correct sequence of interface and propagation matrices, starting with the last interface and working backwards from the direction of propagation. The result is a single 2×2 matrix, T, the transfer matrix of the structure.

The structure can be extended to include multiple layers of thicknesses $s_{j=2}, s_3 ..... s_{m-1}$ and refractive indices $n_2, n_3 ..... n_{m-1}$, as shown in Figure 2 A transfer matrix for the whole structure can be constructed, one that links the forward and backward amplitudes for the fields on either side, by calculating the individual propagation and interface matrices and multiplying them together in the reverse order:

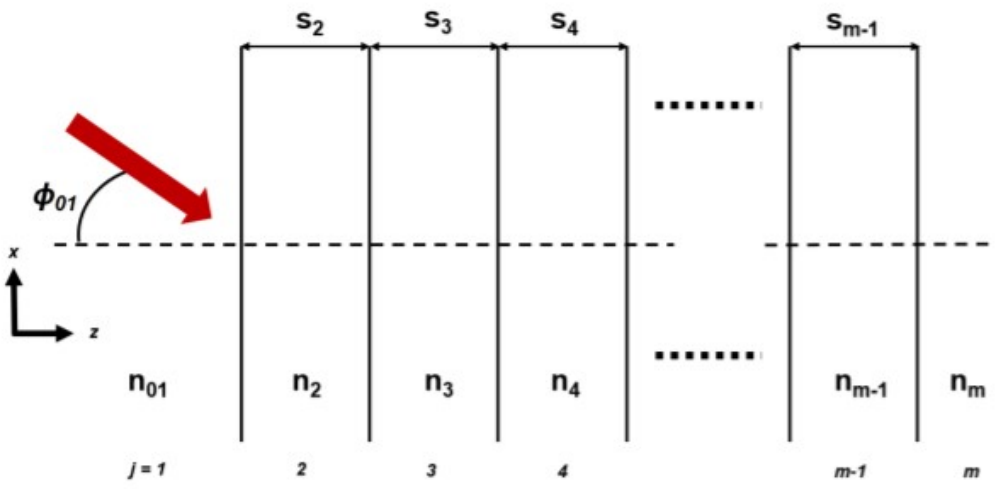

Figure 2: Diagram of a multiple-layer structure [2]

$$\vec{E}_{01} = T\vec{E}_m = \left(\prod_{j=2}^{m-1} I_{(j-1),j} L_j\right) I_{(m-1),m} \vec{E}_m$$

where L_j is the propagation matrix through layer j

$$L_j = \begin{bmatrix} e^{-i\Phi_j} & 0 \\ 0 & e^{i\Phi_j} \end{bmatrix}$$

and $I_{j,j+1}$ is the interface matrix connecting the field amplitudes across the interface between layer j and $j+1$

$$I_{j,j+1} = \left(\frac{1}{t_j}\right) \begin{bmatrix} 1 & r_j \\ r_j & 1 \end{bmatrix}$$

where $\phi_j = k_{jz} s_j = n_j (w/c) q_j s_j$ is the phase thickness of layer j perpendicular to the interface, q_j is the cosine of angle ϕ_j in layer j, and r_j and t_j are the complex Fresnel coefficient of reflection and transmission at the interface between layer j and $j+1$. For TE waves these are

$$r_j = \frac{n_j q_j - n_{j+1} q_{j+1}}{n_j q_j + n_{j+1} q_{j+1}}$$

$$t_j = \frac{2 n_j q_j}{n_j q_j + n_{j+1} q_{j+1}}$$

and for TM waves

$$r_j = \frac{n_{j+1} q_j - n_j q_{j+1}}{n_{j+1} q_j + n_j q_{j+1}}$$

$$t_j = \frac{2 n_j q_j}{n_{j+1} q_j + n_j q_{j+1}}$$

Once a transfer matrix has been calculated for the whole structure it can be used to find its reflection and transmission coefficients. Consider the case of light entering from one side of a structure, with an incoming amplitude defined as 1 and reflection and transmission amplitudes r and t.

$$\begin{bmatrix} 1 \\ r \end{bmatrix} = T \begin{bmatrix} t \\ 0 \end{bmatrix} = \begin{bmatrix} T_{11} & T_{12} \\ T_{21} & T_{22} \end{bmatrix} \begin{bmatrix} t \\ 0 \end{bmatrix}$$

$$r = \frac{T_{21}}{T_{11}}$$

$$t = \frac{1}{T_{11}}$$

Therefore, the elements in the transfer matrix can be used to express the amplitude reflection and transmission coefficients for the total system. The power coefficients are calculated

$$R = \left| \frac{T_{21}}{T_{11}} \right|^2$$

$$T = \frac{n_m q_m}{n_{01} q_{01}} \left| \frac{1}{T_{11}} \right|^2$$

4. Photonic Crystals

Photonic crystals are structures with regular periodic variations in refractive index that affect the propagation of photons in a way analogous to how the periodic potential in a semiconductor crystal lattice affects the motion of electrons. Just as electrons in crystalline atomic lattices encounter bands of energy values they are forbidden from having, so too are photons in photonic crystals forbidden from having certain frequencies (energies), called a photonic bandgap. Because these frequencies cannot propagate through the structure, this is manifested as a spectral window where reflectivity is close to unity (called the stopband).[2]

An example structure is shown in Figure 3 consisting of layers with thickness a and b and refractive index n_a and n_b. The DBR stopband can be intuitively understood as an interference effect. At each interface there is a partial reflection that imparts a phase change on the reflected component. If the optical thickness of the layers are a

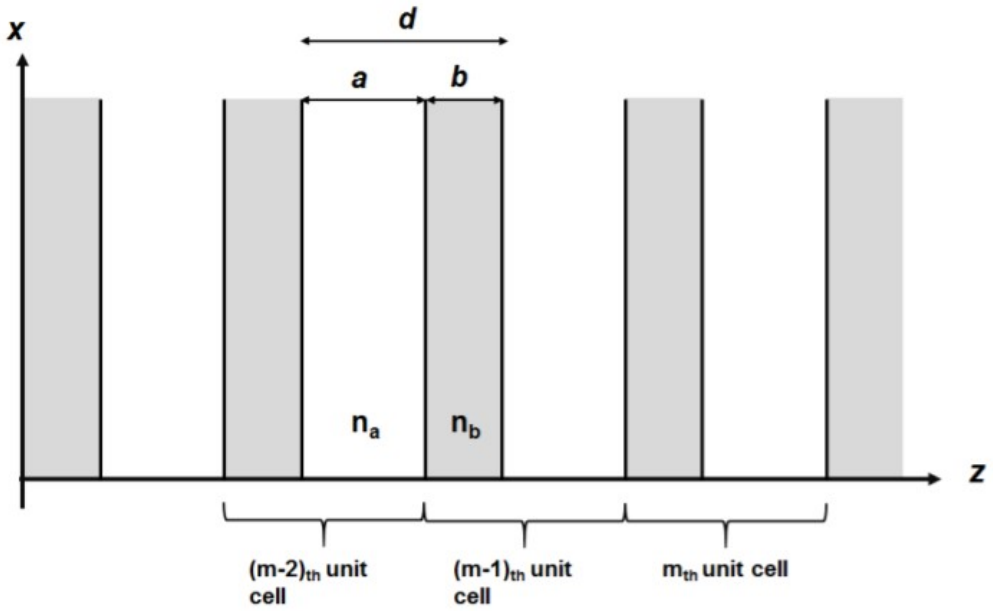

Figure 3: Diagram of periodic layered structure

quarter-wavelength ($= \lambda/4n$) these components interfere constructively in the reflected direction. However, to understand how the DBR can form surface states it is necessary to understand more precisely the propagation of electromagnetic waves in these media. Fortunately, this theory has much in common with the quantum theory of electrons in solids .

The motion of electrons in a solid is given by the Schrödinger equation

$$\left[\vec{\nabla}^2 + (E - V(\vec{r}))\right]\psi(\vec{r}) = 0$$

while the propagation of photons (assuming source-free, harmonic time dependence, etc.) is given by the wave equa

$$\nabla^2\vec{F} + \kappa_0^2\epsilon\vec{F} = 0$$

These are both eigenvalue equations for E and k_o^2 respectively, and both share the same linear form (the curl term can be intuitively considered to correspond to the 'kinetic energy' and ϵ to the 'potential'; photons in higher ϵ material will have a lower potential. Further defining of our geometry (here considering the TE mode) led to

$$\frac{d^2E(z)}{dz^2} + \kappa(z)^2E(z) = 0$$

where $k^2 = (k_o^2\epsilon(z) - \beta^2)$. Like $V(z)$ in a one-dimensional periodic crystal lattice, the permittivities in a DBR also have a periodic function

$$\epsilon(z) = \epsilon(z + d)$$

where $d = a + b$. Above Equation therefore now takes the form of a set of differential equations whose solutions (in one dimension) were first found by Floquet's theorem and, while studying electrons in crystals, more generally by Felix Bloch in 1928, known as Bloch (or Bloch-Floquet) theorem. This states that the solutions must be of the form

$$E(z) = E_K(z)e^{iKz}$$

where $E_K(z)$ is a periodic function with period d and K is the Bloch wavevector. These are known as Bloch waves and form the basis of possible eigenmodes [53]. It should be briefly noted that K is not unique; it can be shown that the periodic component $E_K(z) = E_{K+nG}(z)e^{inGz}$, where $G = 2\pi/d$ is the reciprocal lattice vector and n is an integer number. Just as the Bloch wave is spatially invariant with period d it is also invariant in the reciprocal space with a period G. However, because these have the same solutions it is only necessary to find the eigenmode for each particular K value in the first cell of the reciprocal lattice (n = 1) and this region, called the first Brillouin zone, contains a complete set of all the possible eigensolutions.

The exponential in above equation describes a plane wave envelope when K is a real number, which is a requirement to describe modes in the bulk of the DBR. Complex values of K, which describe exponentially growing or decaying modes, cannot satisfy the

BCs for an infinite DBR since the field will not decay as $|z| \to \infty$. It will be shown later that these correspond to the forbidden stopbands of the DBR. However, it will be demonstrated in chapter 3 that these are also key to the formation of Tamm states.

For now, it is useful to introduce a translation operator T for one unit cell. Using the TMM (section 2.4.1) a translation matrix that links the field amplitudes of the forward and backward propagating waves at equivalent points across a single unit cell of the form

$$\vec{E}(z) = T\vec{E}(z+d) = I_{a,b}L_bI_{b,a}L_a\vec{E}(z+d)$$

which has matrix elements

$$T_{11} = e^{-i\phi_a}\left(cos(\phi_b) - \frac{i}{2}\left[\frac{\kappa_{b,z}}{\kappa_{a,z}} + \frac{\kappa_{a,z}}{\kappa_{b,z}}\right]sin(\phi_b)\right)$$

$$T_{12} = e^{i\phi_a}\left(-\frac{i}{2}\left[\frac{\kappa_{b,z}}{\kappa_{a,z}} - \frac{\kappa_{a,z}}{\kappa_{b,z}}\right]sin(\phi_b)\right)$$

$$T_{21} = e^{-i\phi_a}\left(\frac{i}{2}\left[\frac{\kappa_{b,z}}{\kappa_{a,z}} - \frac{\kappa_{a,z}}{\kappa_{b,z}}\right]sin(\phi_b)\right)$$

$$T_{22} = e^{i\phi_a}\left(cos(\phi_b) + \frac{i}{2}\left[\frac{\kappa_{b,z}}{\kappa_{a,z}} + \frac{\kappa_{a,z}}{\kappa_{b,z}b}\right]sin(\phi_b)\right)$$

where $\phi_a = k_{a,z}a$ and $\phi_b = k_{b,z}b$

$$E(z+d) = E_K(z+d)e^{iKz}e^{iKd} = E(z)e^{iKd}$$

since $E_K(z)$ is periodic. Comparing with the above, it's clear that the Bloch wave must satisfy the eigenvalue problem

$$T\vec{E} = e^{-iKd}\vec{E}$$

where e^{-iKd} are the eigenvalues of the translation matrix T. Using the fact T is unimodular these are shown to be

$$e^{-iKd} = \frac{1}{2}(T_{11} + T_{22}) \pm \sqrt{\frac{1}{4}(T_{11} + T_{22})^2 - 1}$$

This gives the dispersion relation for the Bloch wave

$$\cos(Kd) = \frac{T_{11} + T_{22}}{2}$$

The corresponding eigenvectors for are

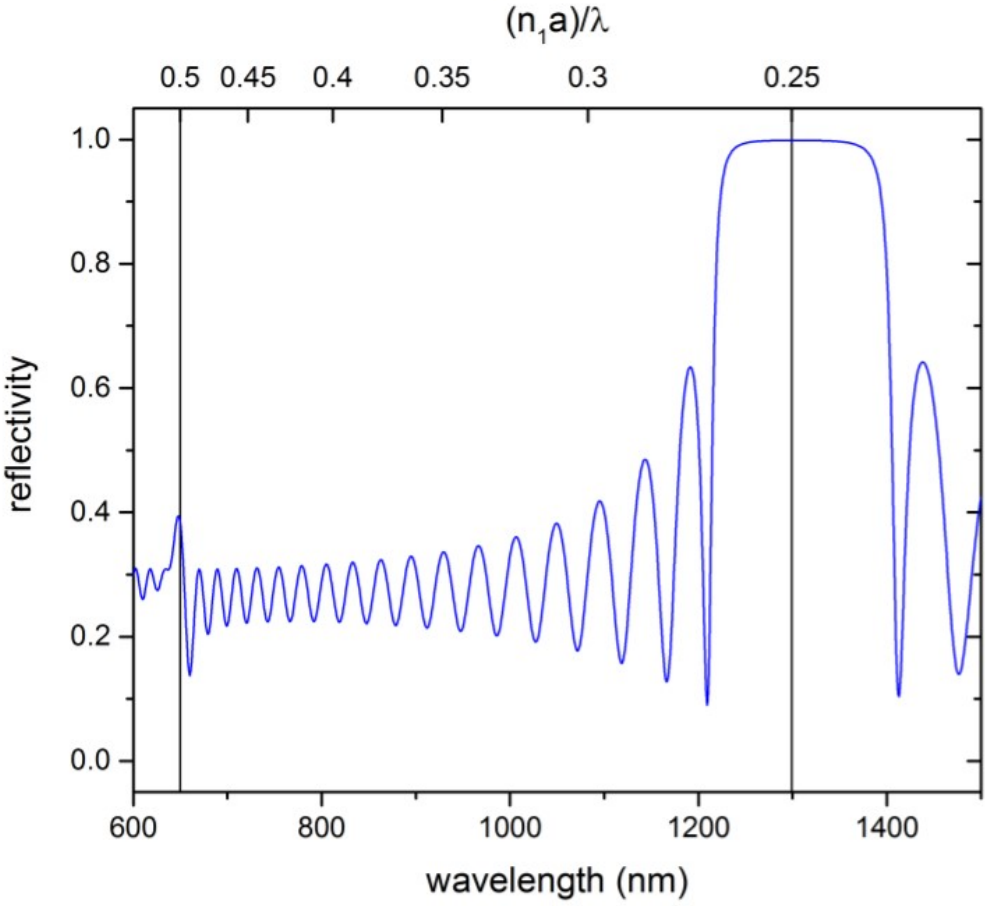

Figure 4: : Reflectivity spectra for an 18x pair /4 DBR with a photonic stopband centered on 1300 nm ($n_1 = 3.5, n_2 = 2.9$), showing the first band edge and photonic stopband as a function of wavelength and ($n_1 a/\lambda$). Calculated using the transfer matrix method [2]

$$\vec{u}_0 = \begin{bmatrix} v_0 \\ w_0 \end{bmatrix} E_K(z) = \begin{bmatrix} T_{12} \\ e^{-iKd} - T_{11} \end{bmatrix} E_K(z)$$

An example DBR for telecoms wavelength is shown in Figure 4 consisting of 18x pairs of $n_a = 3.5$, $n_b = 2.9$, $a = 95nm$ and $b = 110nm$. Both show the reflection power coefficients at normal incidence to the DBR. The photonic stopband is the window of high reflectivity between 1230 and 1380 nm.

4.1. ***Simulation of Photonic crystal***

Simulated reflectivity graph for s and p-polarization at certain angle is added in the below discussion. Along with reflectivity, electric field evolution inside the DBR is also simulated.

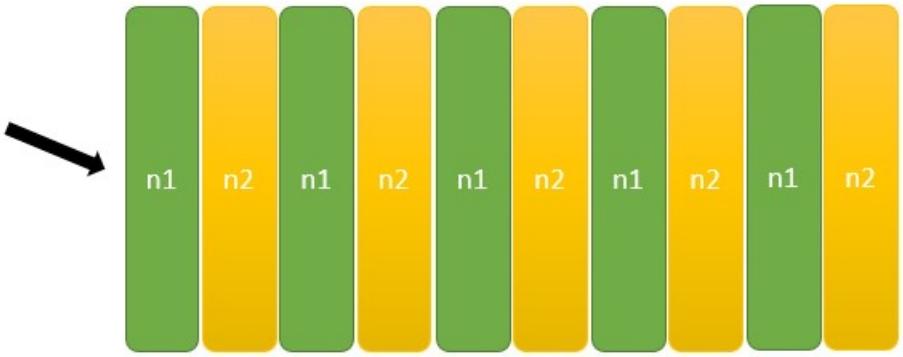

Figure 5: Distributed bragg reflectors (DBR), 10 bilayers, $n_1 = 1.465$ and $n_2 = 2.869$ with $d1 = 106nm$ and $d2 = 150nm$

- S-polarization
- At 60^o incidence
- 10 bilayers, $n_1 = 1.465$ and $n_2 = 2.869$ with $d1 = 106nm$ and $d2 = 150nm$
- Reflectivity spectrum : Figure 6(1)
- Electric field evolution for $580nm$ wavelength(Figure 6(2)).
- Electric field evolution for $700nm$ wavelength(Figure 6(3)).

- P-polarization
- At 60^o incidence
- 10 bilayers, $n_1 = 1.465$ and $n_2 = 2.869$ with $d1 = 106nm$ and $d2 = 150nm$
- Reflectivity spectrum : Figure 7(1)
- Electric field evolution for $580nm$ wavelength(Figure 7(2)).
- Electric field evolution for $700nm$ wavelength(Figure 7(3)).

5. Tamm plasmons

Surface state can be excited at the interface of a DBR and a metal below its plasma frequency. - the confinement in the metal layer is due to its negative permittivity - they are confined into the DBR by its photonic stopband (as opposed to by TIR in the SPP). These modes are called Tamm plasmons polaritons, or Tamm plasmons (TPs). Because the dispersion curves are within the light line they can be directly excited by light incident on the air side, with no need for prism-coupling or gratings.[2]

Since the DBR can also act as a NMP material TPs can be excited in TE and TM polarization (note that the layer adjacent to the metal, the spacer, is still $\epsilon > 0$ and

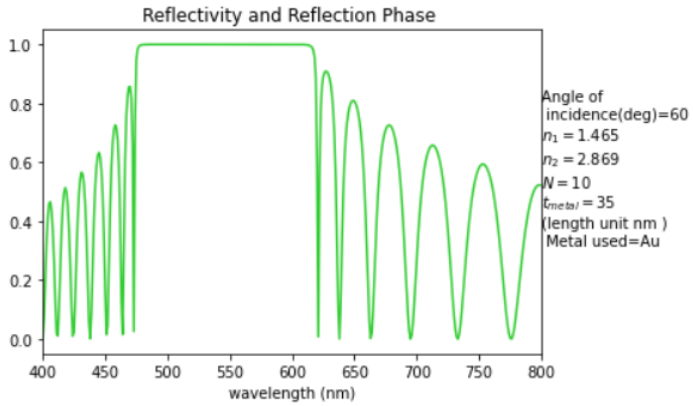

Figure 1: Reflectivity spectrum for S-polarization

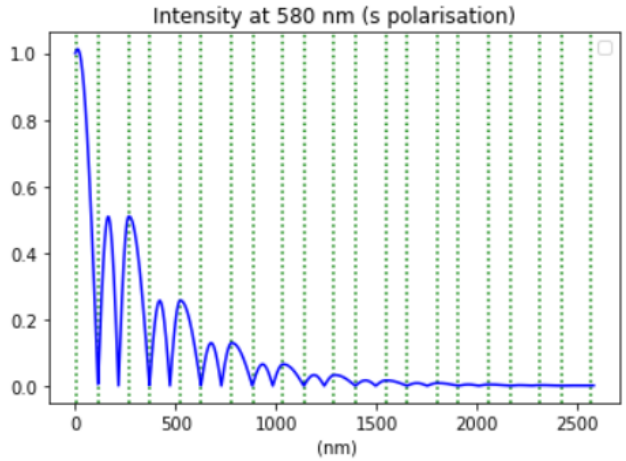

Figure 2: Electric field for $\lambda = 580nm$

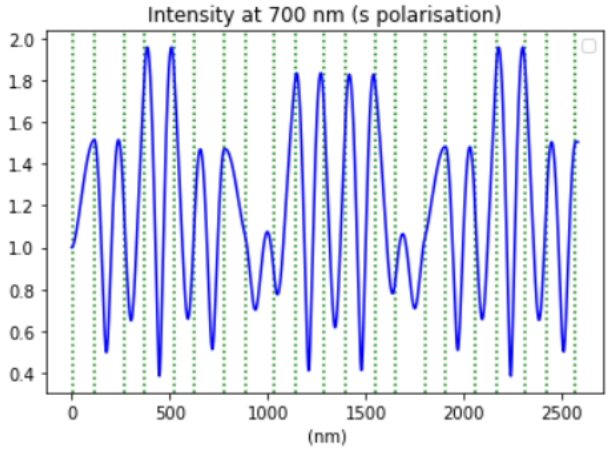

Figure 3: Electric field for $\lambda = 700nm$

Figure 6: Electric field evolution for two wavelength(one inside the bandgap and one outside)

$\mu > 0$; it is only effectively negative in the stopband with respect to light propagating normal to the DBR periodicity. This combination allows the matching conditions at the interface to be met simultaneously with the decaying solutions required of a surface modes). The condition for a Tamm plasmon becomes

$$r_M r_{PhC} = 1 \tag{11}$$

where r_{PhC} is the amplitude reflection coefficient of light incident on the DBR surface, which is given by section(3), and $r_M = (n_a - n_M)/(n_a + n_M)$ is the amplitude reflection coefficient of the metal. Using the Drude equation, in cases below the metal plasma frequency (i.e. $\omega_p^2 >> \omega^2$) when $n_M \approx i\frac{\omega_P}{}$.

$$r_M \approx -1 - \frac{2in_a\omega}{\omega_p} \approx -e^{\frac{2in_a\omega}{\omega_p}} = e^{[i(\pi + \frac{2n_a\omega}{\omega_p}]}$$

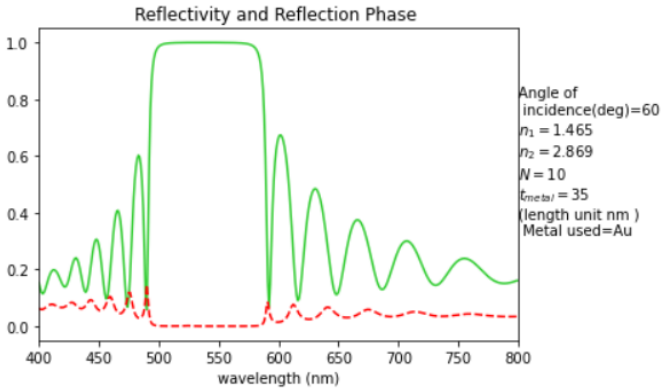

Figure 1: Reflectivity spectrum for P-polarization

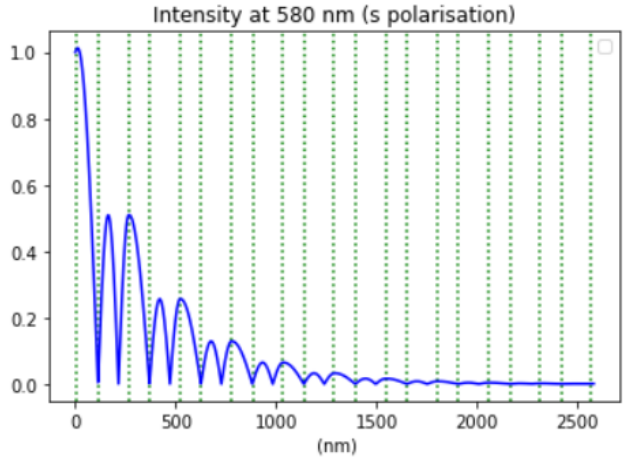

Figure 2: Electric field for $\lambda = 550nm$

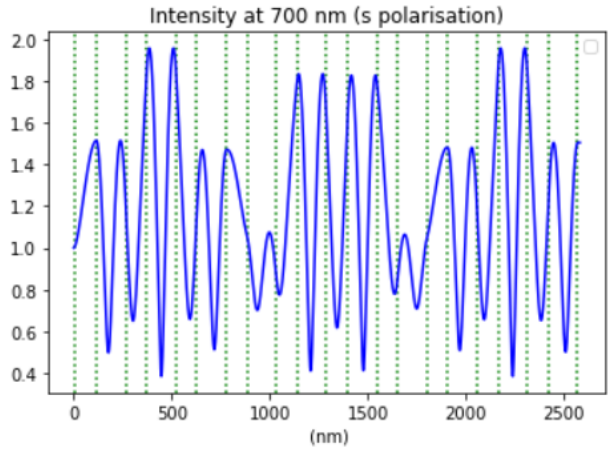

Figure 3: Electric field for $\lambda = 700nm$

Figure 7: Electric field evolution for two wavelength(one inside the bandgap and one outside)

An example TP(Tamm Plasmon) structure is shown in Figure 8 and the calculated reflectivity at normal incidence for a 17.5x pair GaAs/AlAs ($d_1 = 95nm$ and $d_2 = 110nm$) DBR, a $75nm$ GaAs spacer layer and $25nm$ gold layer is shown in Figure 8(b) When the metal is removed a photonic stopband is clearly visible between $1205nm$ and $1375nm$. When the gold film is added (red line) the TP can be seen by the appearance of a dip in the reflectivity spectrum centered at $\lambda = 1300nm$, where the light now couples into the Tamm mode.[2]

5.1. ***Simulation of Tamm states***

Now, a metal-coated photonic crystal (PhC) is considered. A resonant wavelength is observed where there is maximum absorption i.e. reflectivity spectrum exhibits a significant dip and corresponding transmission is not seen. This phenomenon is surface plasmon resonance and such optical state of the surface are also known as tamm states which occur due to a phase matching criteria. Here, using computation, the criteria for

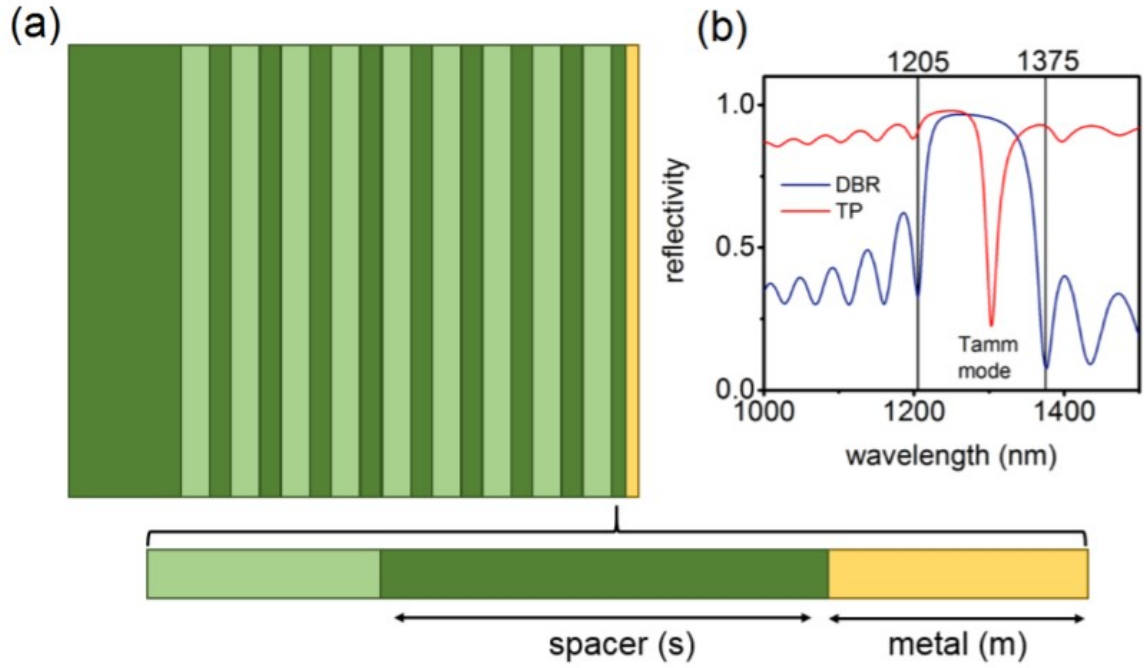

Figure 8: (a) Diagram of a Tamm plasmon structure. (b) Calculated reflectivity spectra at normal incidence for a 17.5x pair GaAs/AlAs DBR, GaAs spacer (s = 75 nm) and with (red line) and without (blue line) m = 25 nm gold layer. Black lines show the first minima of the DBR stopband. The TP mode can be seen as a dip in reflectivity within the stopband. Calculated using TMM [2]

observing Tamm states is studied.

5.1.1. ***Surface Plasmon Resonance - using Gold*** Consider the case where light falls like : $Light \rightarrow Metal \rightarrow PhC$.

$Light \rightarrow Metal \rightarrow n_1\ n_2\ n_1\ n_2$....

Gold of 30nm thickness is coated on the incidence surface and spectrum was simulated. Figure 9(1) shows the model considered for the simulation. Next we have plotted reflection (Black curve) and transmission (Red curve) curves in Figure 9(2) We also added photonic crystal reflection curve (Grey curve) in Figure 9(2) for the comparison. We know for gold plasma wavelength $\lambda_p = 168nm$ and collision wavelength $\lambda_c = 8934nm$ [3], we used these wavelength information to calculate varying reflective index of gold.

- S-polarization
- At 60^o incidence
- 10 bilayers, $n_1 = 1.465$ and $n_2 = 2.869$ with $d1 = 106nm$, $d2 = 150nm$ and $d_{metal} = 35nm$
- Reflectivity spectrum : Figure 10(1)

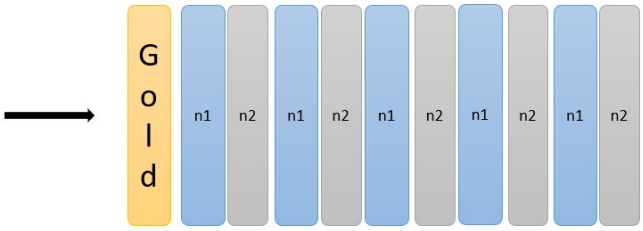

Figure 1: Schematic diagram of system

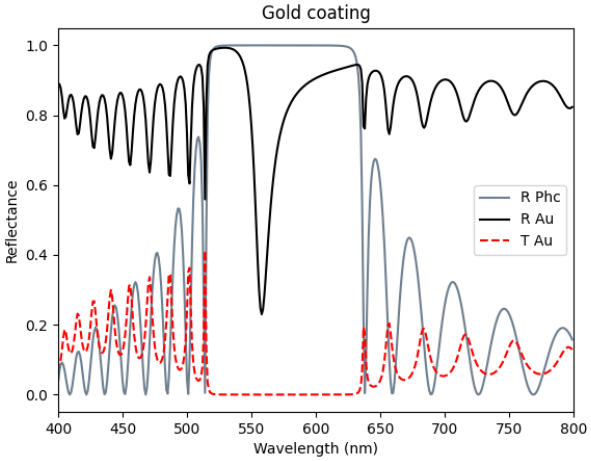

Figure 2: Reflection (Black curve), transmission (Red curve) and PhC reflection (Grey curve) curves

Figure 9: $Light \rightarrow Metal \rightarrow PhC$. Gold of 30nm thickness is cotted on 10 bilayers, $n_1 = 1.5$ and $n_2 = 2.8$ with $d1 = 100nm$ and $d2 = 150nm$

- Electric field evolution for $559nm$ wavelength(Figure 10(2)).
- Electric field evolution for $690nm$ wavelength(Figure 10(3)).

Now for the P-polarization we can find the simulation details below

- P-polarization
- At 60^o incidence
- 10 bilayers, $n_1 = 1.465$ and $n_2 = 2.869$ with $d1 = 106nm$, $d2 = 150nm$ and $d_{metal} = 35nm$
- Reflectivity spectrum : Figure 11(1)
- Electric field evolution for $525nm$ wavelength(Figure 11(2)).
- Electric field evolution for $700nm$ wavelength(Figure 11(3)).

Consider the case where light falls like : $Light \rightarrow PhC \rightarrow Metal$.
$Light \rightarrow n_1\ n_2\ n_1\ n_2.... \rightarrow Metal$

- S-polarization (Metal on the right side)
- At 60^o incidence
- 10 bilayers, $n_1 = 1.465$ and $n_2 = 2.869$ with $d1 = 106nm$, $d2 = 150nm$ and $d_{metal} = 35nm$
- Reflectivity spectrum : Figure 12(1)
- Electric field evolution for $642nm$ wavelength(Figure 12(2)).
- Electric field evolution for $720nm$ wavelength(Figure 12(3)).

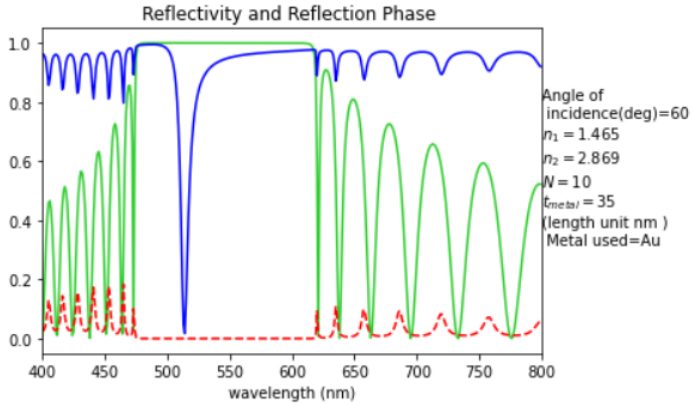

Figure 1: Reflectivity spectrum for S-polarization (Metal)

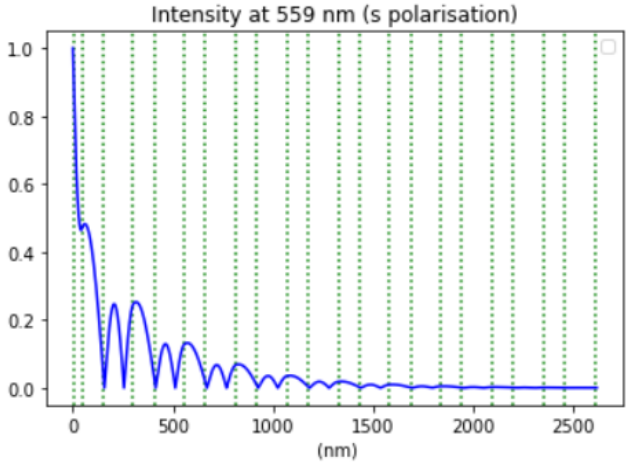

Figure 2: Electric field for $\lambda = 559nm$

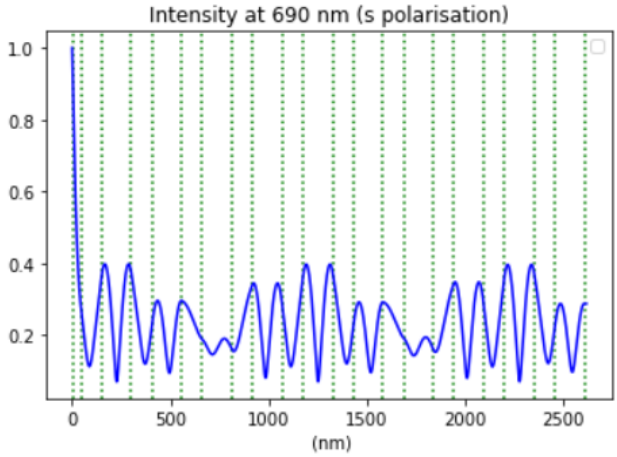

Figure 3: Electric field for $\lambda = 690nm$

Figure 10: Electric field evolution for S-polarization (Metal coated on the left side of DBR)

- P-polarization (Metal on the right side)
- At 60^o incidence
- 10 bilayers, $n_1 = 1.465$ and $n_2 = 2.869$ with $d1 = 106nm$, $d2 = 150nm$ and $d_{metal} = 35nm$
- Reflectivity spectrum : Figure 13(1)
- Electric field evolution for $534nm$ wavelength(Figure 13(2)).
- Electric field evolution for $750nm$ wavelength(Figure 13(3)).

6. Conclusion

The analogy between a system with periodic potential in Condensed Matter Physics and the photonic band gap in Optics has been extensively investigated in order to develop

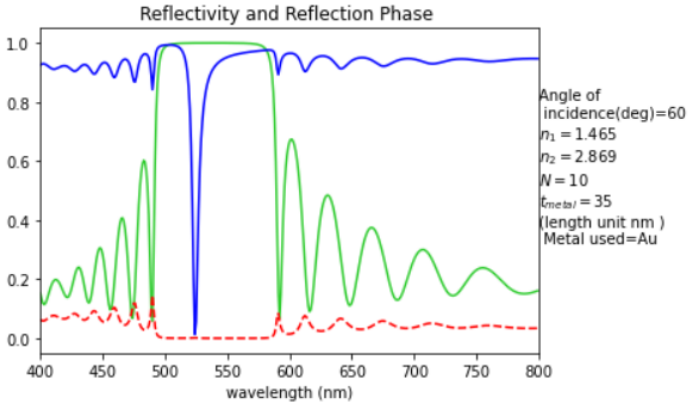

Figure 1: Reflectivity spectrum for P-polarization (Metal)

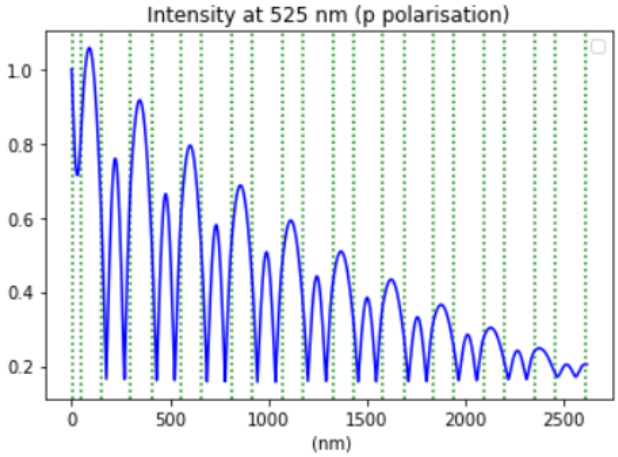

Figure 2: Electric field for $\lambda = 525nm$

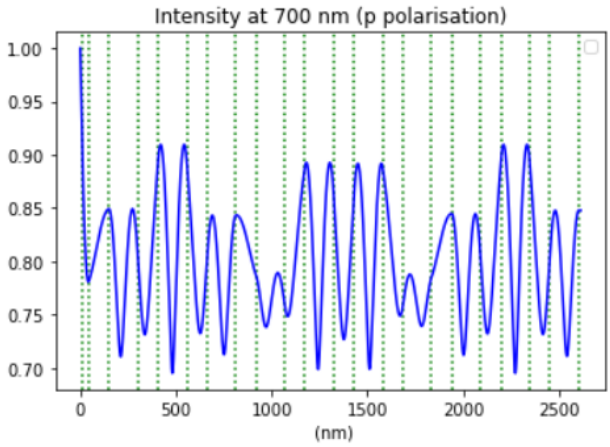

Figure 3: Electric field for $\lambda = 700nm$

Figure 11: Electric field evolution for P-polarization(Metal coated on the left side of DBR)

a theoretical foundation for Surface states seen in periodic arrangements of dielectrics with varying refractive indices. This comparison offers up new avenues for studying Surface Plasmons, as well as designing experiments and developing computer modelling that can help us better understand the mechanics of interface states.

Further ideas that can be explored via this experiment can "Tamm plasmon-coupled emission", "Confined Tamm plasmons", "DBR-DBR mode confinement" and "Symmetry broken DBR" etc. The parameters in the control during simulation were refractive indices, no. of bilayers, thickness of each layer, thickness of metal coated and position of incident light. These allowed us to extensively simulate various results and establish and predict relations in symmetric cases. The conditions for obtaining surface plasmon resonance were explored. Specifically, the dependence of Angle of Incidence on the Tamm resonant wavelength is studied for both s (TE Mode) and p-Polarisation (TM Mode).

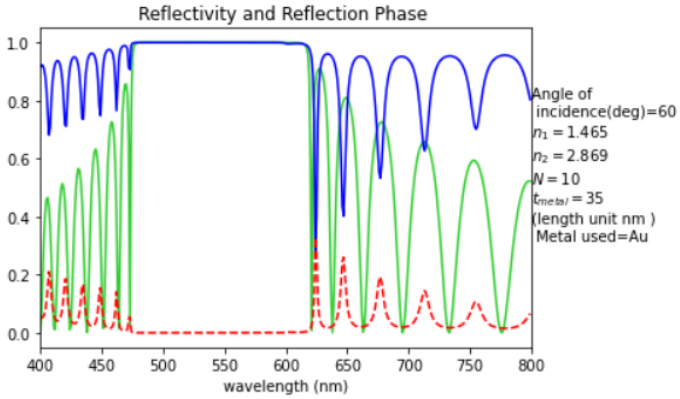

Figure 1: Reflectivity spectrum for S-polarization (Metal)

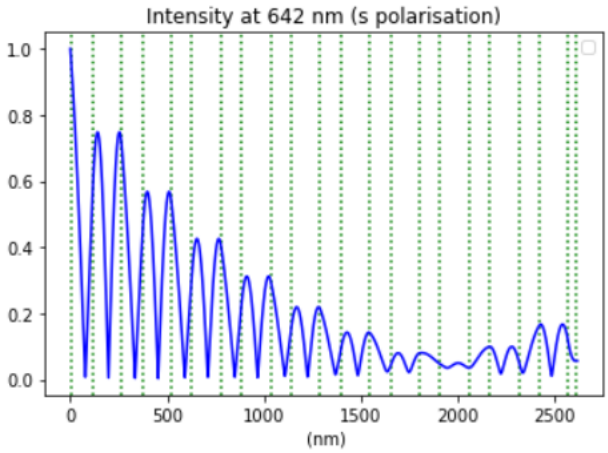

Figure 2: Electric field for $\lambda = 642nm$

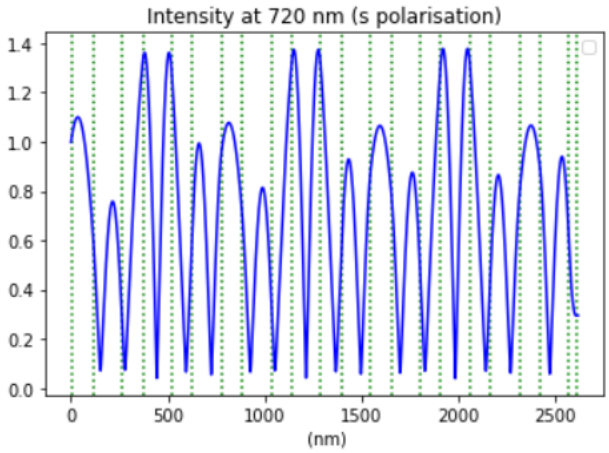

Figure 3: Electric field for $\lambda = 720nm$

Figure 12: Electric field evolution for S-polarization (Metal coated on the right side of DBR)

References

[1] Danni Hao. Hybridisation of plasmonic and acoustic biosensing devices. (1), 2017. URL `http://theses.gla.ac.uk/8992/`.

[2] Matthew Parker. Optical tamm states for novel optical and quantum optical devices. *University of Bristol*, (1), 2017. URL `https://research-information.bris.ac.uk/ws/portalfiles/portal/186573348/Final_Copy_2019_01_23_Parker_M_PhD.pdf`.

[3] Sarika Singh and B D Gupta. Simulation of a surface plasmon resonance-based fiber-optic sensor for gas sensing in visible range using films of nanocomposites. *IOP PUBLISHING*.

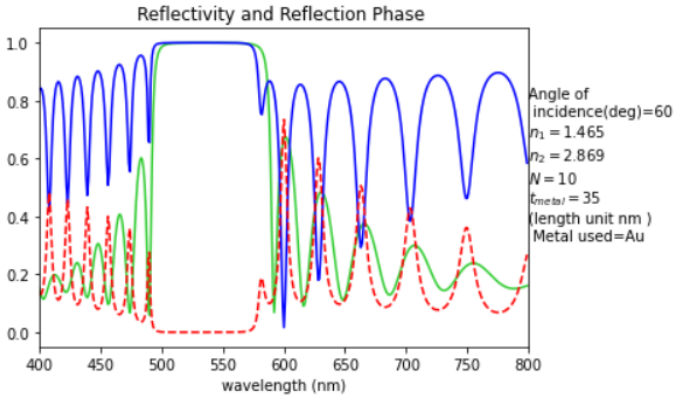

Figure 1: Reflectivity spectrum for P-polarization (Metal)

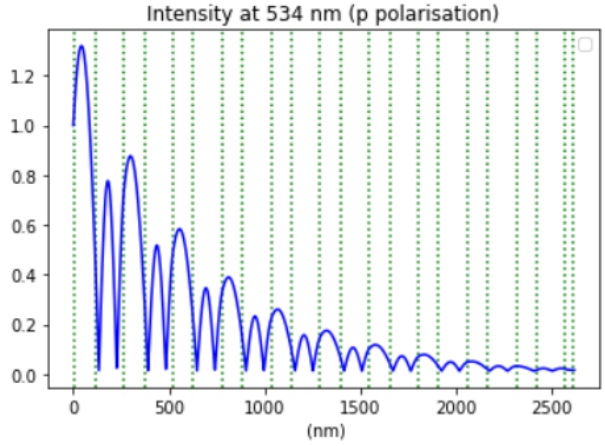

Figure 2: Electric field for $\lambda = 534nm$

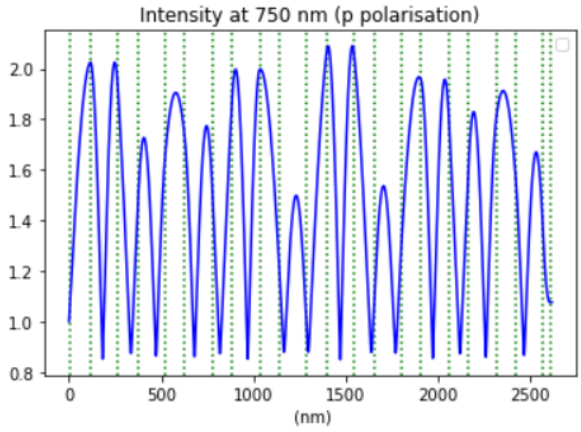

Figure 3: Electric field for $\lambda = 750nm$

Figure 13: Electric field evolution for P-polarization(Metal coated on the right side of DBR)